Tribology International 167 (2022) 107418

Contents lists available at ScienceDirect

Tribology International

journal homepage: www.elsevier.com/locate/triboint

The nature of atomic wear from molecular simulations

Yongjian Yang [a], Corey S. O'Hern [b], Liping Huang [a], Yunfeng Shi [a,*]

[a] Department of Materials Science and Engineering, Rensselaer Polytechnic Institute, Troy, NY 12180, USA
[b] Mechanical Engineering & Materials Science, Applied Physics, and Physics, Yale University, New Haven 06520, USA

ARTICLE INFO

Keywords:
Atomic wear
Athermal activation
Single-asperity sliding
Molecular dynamics

ABSTRACT

Atomic wear is generally understood as a mechanically-assisted and thermally-activated bond-breaking chemical process. In other words, debris formation is proportional to time just like a chemical reaction (instead of sliding distance), the contact area, and strongly temperature-dependent. Here using molecular dynamics, we show in a model glassy tribo-system at relatively high sliding speeds that the atomic wear depends weakly on the temperature and not on the sliding speed and increases sub-linearly with the contact area. We propose a different wear formulation for this system by considering that the debris-formation process at relatively high sliding speed is shear-assisted and athermally-activated.

1. Introduction

Sliding between surfaces is ubiquitous in man-made machines, biological and geological systems. The paramount question in all tribological processes is to determine the mechanical resistance from dissipation (friction) and material loss (wear). Unlike friction, a subject of investigation since the times of the Ancient Greeks, wear is much less understood. Archard established the macroscopic adhesive wear law half century ago[1]; however, Archard's linear wear law is far from universally applicable in terms of material systems and loading regime. Recently, microscopic debris generation has received increasing interests, driven by the tremendous advancement in fabrication of nano-scale devices and the need for quantitative reliability assessment. For example, a better understanding of nano-scale wear has been achieved in both high speed sliding systems, e.g. the head/disk interface of hard drives (~10 m/s)[2,3], and low speed sliding systems, e.g. atomic force microscope (AFM) probes for high-density data storage (<1.5 mm/s)[4,5]. Microscopic wear at the contacting surfaces is distinct from macroscopic debris formation [6]: (1) interfacial adhesion is much stronger compared to the weight of the device at the nanoscale [7]; (2) continuum mechanics breaks down at the atomic scale [8]; (3) contacts contain just one or few single-asperity joints (e.g. in AFM). A new wear mechanism, atomic wear, has been identified in single-asperity sliding experiments at very low loads by different groups [4,5,9,10,11]. Based on this mechanism, the wear rate is an exponential function of the contact stress, deviating from Archard's linear wear law.

A number of analytical models have been proposed for atomic wear [4,9,10] of single-asperity which are critical to understand wear in multi-asperity contact [1]. These models are all based on the notion that atomic wear is a thermally activated and mechanically assisted bond rupture process. The wear rate can be expressed using an Eyring-like formula as [4,9–15],

$$\frac{\Gamma_{debris}}{\Gamma_{attempt}} = \exp\left(-\frac{E_a - \sigma V_{act}}{k_B T}\right), \tag{1}$$

where $\Gamma_{attempt}$ is the number of debris generation attempts per unit area per unit time, Γ_{debris} is the number of debris generation events per unit area per unit time, k_B is the Boltzmann constant, and T is the thermodynamic temperature. E_a is the activation energy, which is reduced by the stress σ conjugate to the activation volume V_a. The wear rate can be also written in terms of the debris volume V_{debris} per sliding distance L,

$$\frac{dV_{debris}}{dL} = \frac{A \cdot \Gamma_{attempt} \cdot \exp\left(-\frac{E_a - \sigma V_{act}}{k_B T}\right) v_m}{v_s}, \tag{2}$$

where A is the contact area, v_m is the molecular volume, and v_s is the sliding speed. The conversion from Eq. 1 to Eq. 2 builds upon the proportionality between the sliding distance (L) and the time (t) via the sliding speed (v_s).

We have shown the exponential dependence of the atomic wear on the stress in our previous study of a Lennard-Jones system [16], however, the applicability of the above formulation in such system has not been verified in the dependence of the wear rate on the sliding speed and

* Corresponding author.
E-mail address: shiy2@rpi.edu (Y. Shi).

https://doi.org/10.1016/j.triboint.2021.107418
Received 8 October 2021; Received in revised form 25 November 2021; Accepted 21 December 2021
Available online 24 December 2021

Table 1
Summary of simulation conditions. Specific conditions can be found in the caption of each figure presented.

Simulation models	Tip size (nm)	# total atoms	Velocity, v_0 (m/s)	Adhesion strength, κ	Temperature (K)	Normal/frictional stress (GPa)
Sliding simulations (Section 2.2)	l_x: 3–33 l_y: 4[a] l_z: 5	$8 \times 10^3 \sim 1.1 \times 10^5$	0.012 ~ 37	0.1~ 0.25	$T_{kinetic}$: 30 ~ 650	σ_n: 0.2 ~ 1.0
T_{eff} measurement (Section 2.3)	l_x: 5 l_y: 4 l_z: 15	2×10^4	12	0.25	$T_{kinetic}$: 60 ~ 350	σ_n: 0.05 ~ 0.1
GLD simulations (Section 2.4)	l_x: 5 l_y: 1 l_z: 5	2×10^3	11[b]	0.2[c]	$T_{kinetic}$: 63 T_{eff}: 1050 ~ 4400	σ_n: 0.3 ~ 1.2 σ_f: 0.2 ~ 0.9

[a] Because only a thin layer of tip atoms are participating the atomic wear process and the wear rate can be extremely low [16], a small tip height (l_y) was used to facilitate long-time sliding simulation and wear rate measurement.
[b]The velocity is calculated by dividing the atomic roughness (0.27 nm) with the characteristic τ_k 25 *ps* adopted in GLD simulations.
[c] The tip is pressed by a flat wall which interacts with the tip atoms with a Lennard-Jones 9–3 potential. The value 0.2 corresponds to the rescaling factor for the energy of this potential in order to reduce adhesion.

temperature. An often-overlooked issue is that a chemical reaction (the notion behind Eq. 1) is a function of time, while debris formation can depend strongly on sliding distance. Another significant consequence of the current formulation is that the wear rate should be proportional to the contact area under constant contact stress, as bond-breaking events are equivalent to wear. Third, it is not clear which component of the stress tensor should be used in the above equations, as both the shear stress and the normal stress have been used in literatures [9,10,17].

While there are significant expermental limitations in controlling sliding conditions, as well as precise measurements of wear rates in the atomic wear regime, atomistic simulations [16,18,19] can track the motion of all atoms and quantify the wear volume with atomic accuracy

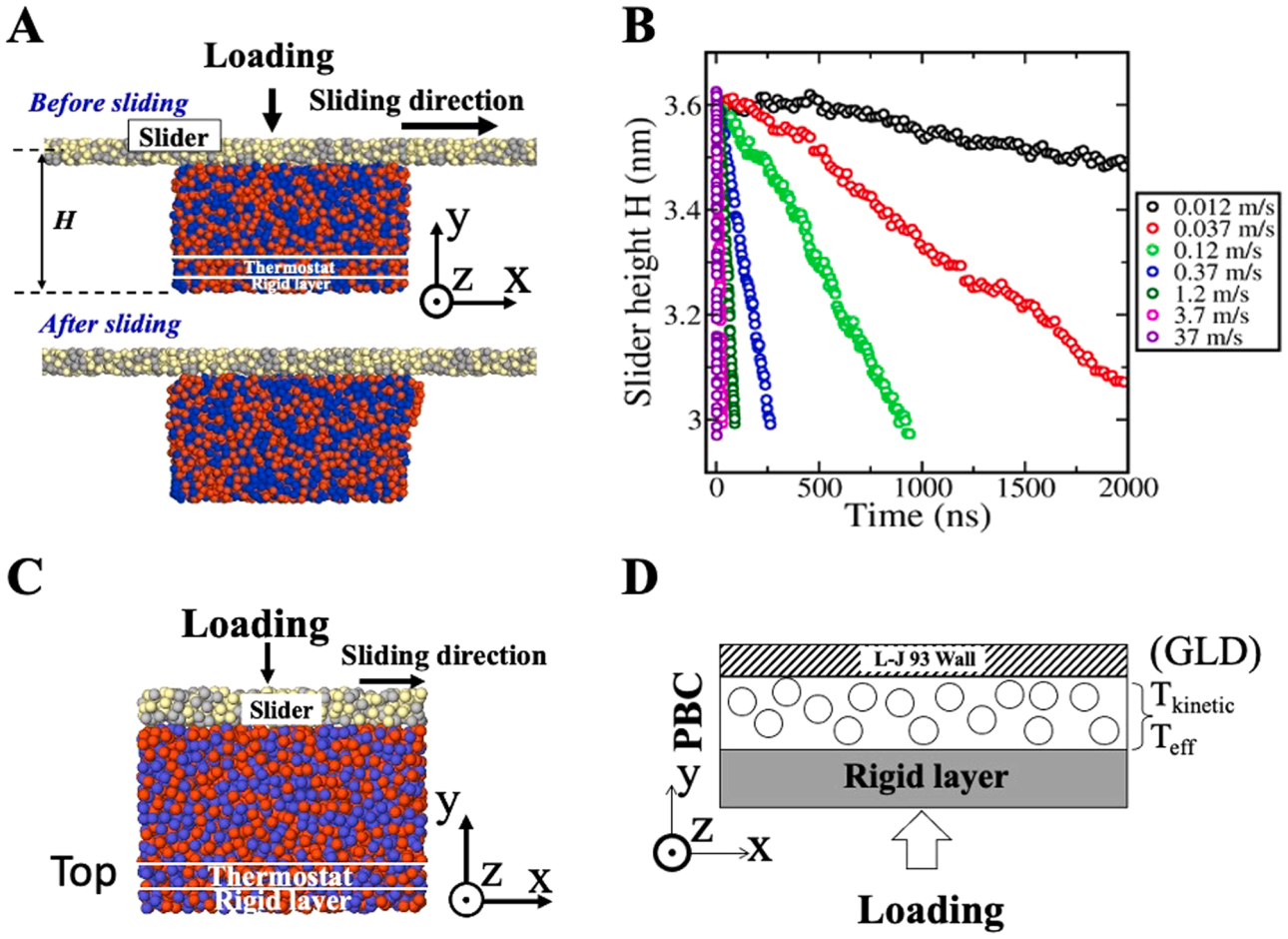

Fig. 1. (A) Side view of the tip wear system before and after sliding 60 nm. The sample is 6 nm long in x-direction. The wear parameters are: $T_{kinetic} = 63$ K, $\kappa = 0.10$, $\sigma_n \approx 0.4$ GPa, $v_0 \approx 12$ m/s. H is the height of the slider. The two-colored atoms in both the slider and the tip correspond to the two types of atoms of the binary Lennard-Jones glass, respectively. (B) Example sliding curves of the slider height H versus the time t at different sliding velocities as noted in the legend. All H–t curves can be linearly fitted with a high correlation coefficient (> 0.98). The sliding conditions are: $\kappa = 0.25$, $T_{kinetic} = 63$ K, $\sigma_n \approx 0.1$ GPa. (C) A cross-sectional view of the tip-wear system used for measuring the effective temperature T_{eff}. (D) Schematic representation of the generalized Langevin dynamics simulations used to model atomic wear. Shear stress is applied to the tip material by superimposing a constant lateral force f in the x-direction. In (A), (C) and (D), periodic boundary conditions (PBC) are applied in the x-z plane. In (A) only the slider is continuous in the x-direction. In contrast, both the slider and the tip are continuous in the x-direction in (C) and (D).

although higher sliding speeds [20–22] and simplified models [22–24] are commonly used as oppose to experiments. In this study, we systematically investigated the tip wear dependence on temperature, sliding velocity, and tip size using molecular dynamics (MD) simulations of a Lennard-Jones model glass. While not intended for chemical systems with strong covalent bonds [4,9,10,19,25,26], L-J model glass is useful to test the applicability of aforementioned wear formula on simple systems with affordable simulation cost. It has been shown the wear mechanism in this model transits from the atomic wear regime to a different wear regime at high contact stress where the wear scales linearly with the contact stress [14,16,18]. Our current results provide further evidence that atomic wear in such system at high sliding speeds is not thermally activated, and debris atoms are re-depositable. We also examined the atomic wear behavior based on athermal activation using generalized Langevin dynamics simulations. We found the atomic wear in the L-J system is mechanically activated and the kinetics can be better described with the concept of effective temperature from non-equilibrium thermodynamics.

2. Methods

2.1. Interatomic force field

We employed a binary Lennard-Jones model to simulate tip wear. Both the tip and the slider are composed of glassy binary alloys interacting via the Wahnström potential [27], as described in our previous work [16,28]. We chose to study an amorphous system, instead of a crystalline one for several reasons: (1) the amorphous sample is isotropic, thus obviating the need to investigate different crystallographic orientations as is the case for crystalline samples; (2) amorphous oxide layers are frequently encountered in single-asperity tips (such as AFM tips). In fact, a number of recent MD simulations of wear have elected to use amorphous samples [16,18,19].

The tip system using the Wahnström potential [27] consists of two species of atoms to bypass crystallization: S for small and L for large atoms, which interact via a binary Lennard-Jones (BLJ) potential of the form,

$$\phi_{ij} = 4\varepsilon_{\alpha\beta}\left[\left(\frac{\sigma_{\alpha\beta}}{r_{ij}}\right)^{12} - \left(\frac{\sigma_{\alpha\beta}}{r_{ij}}\right)^{6}\right], \tag{3}$$

where α and β represent species S or L. $\varepsilon_{\alpha\beta}$ represents the bonding energy, $\sigma_{\alpha\beta}$ provides a length scale (the distance at which the interaction energy is zero), and both are species-dependent. The SS and LL bond energies are equal to that of the SL bond energy so that $\varepsilon_{SS} = \varepsilon_{SL} = \varepsilon_{LL}$. The SS and LL length scales are related to the SL length scale by $\sigma_{SS} = \frac{5}{6}\sigma_{LL}$, $\sigma_{SL} = \frac{11}{12}\sigma_{LL}$. The cutoffs for the *SS, LL, and SL* interactions are $2.08\sigma_{LL}$, $2.5\sigma_{LL}$ and $2.29\sigma_{LL}$, respectively. The cutoffs were chosen such that the potential energy values for the different interactions at their respective cutoffs have the same value $-0.0163\varepsilon_{LL}$. The reference length and energy scales are σ_{LL} and ε_{LL}, respectively. The two types of atoms have different masses such that. The reference time scale is $t_0 = \sigma_{LL}\sqrt{m_0/\varepsilon_{LL}}$. The time step for trajectory integration is 0.01 t_0. The mode coupling temperature, T_{MCT}, was measured to be $0.57\varepsilon_{LL}/k_B$, where k_B is the Boltzmann constant. The internal units in the Wahnstrom system can be converted into physical units using binary metallic glass systems (taking Ni-Nb as an example) [29,30] as follows: $t_0 \approx 0.5$ ps, $\sigma_{LL} \approx 2.7$ Å, $m_0 \approx 46$ amu, and $T_{MCT} \approx 1000$ K. We provide the conversion from Lennard-Jones units to SI units for stress, velocity, and temperature: (stress) $\frac{\varepsilon_{LL}}{\sigma_{LL}^3} \approx 1.23$ GPa; (Sliding velocity) $\sqrt{\varepsilon_{LL}/m_0} \approx 540$ *m/s*; and (temperature) $\varepsilon_{LL}/k_B \approx 1754$ *K*. Quantum effect can be ignored because the de Broglie thermal wavelength (0.32 Å) is much smaller than the interatomic distance and the sliding process takes much longer time than $\hbar/k_BT$, where $\hbar$ is the Planck constant [31].

Based on the BLJ potential, we have conducted sliding simulations with a tip-slider tribo-system, measured the effective temperature of the tribo-system and conducted wear simulations using a toy model with effective temperature controlled by the generalized Langevin dynamics (GLD) thermostat. The setup of different simulations will be described in the following sections. Some common simulation conditions are summarized in Table 1.

2.2. Sliding simulation

A tip wear tribo-system was chosen that mimics an AFM tip sliding on a flat rigid substrate (slider) following previous studies [16,28]. Fig. 1 A shows a side view of the tip wear tribo-system before and after sliding. Because the tapering angle of the conical tip is small in experiments [9,10] and the atomic wear rate is low, for convenience, a rectangular tip is used so that the contact area remains constant during the sliding. The tip has a length (l_x) of 3–33 nm in the sliding x-direction, a height of 4 nm in the y-direction, and a thickness (l_z) of 5 nm in the z-direction. Periodic boundary conditions (PBC) are applied in the x/z-direction and the thickness of the sample in the z-direction is fixed (plane strain condition). To prevent accidental reentering of debris atoms back to the interface with the slider, any tip atoms sticking with the slider and moving far away from the tip would be deleted during the sliding simulation. The bottom layer of 0.8 nm of the tip is held rigid. A layer of 0.6 nm above the rigid layer is coupled to a Nosé -Hoover [32,33] thermostat with a target temperature $T_{kinetic}$ to dissipate heat due to sliding. The rest of the tip is not directly coupled to any thermostat. For the continuous flat slider, atoms are constrained to rigid body motion without atomic vibrations. Both the tip and the slider are binary Lennard-Jones glass interacting via the BLJ potential. The bulk glass samples were created by quenching well-equilibrated liquids from 2100 K to a target temperature $T_{kinetic}$ (30–650 K) using a cooling rate of 0.8 *K/ps*. Tip samples were then cut from the glassy samples.

The tip-slider interaction is controlled by $\varepsilon_{\alpha\beta}^{Tip-Slider} = \kappa\varepsilon_{\alpha\beta}$ ($\alpha, \beta = S$ or L). Here $\varepsilon_{\alpha\beta}$ are the original Wahnström parameters, and κ is a dimensionless parameter used to adjust the interfacial strength. We have previously shown that adhesion (high interfacial strength) suppresses atomic wear [16]. In this work, we adjusted κ to be weak, i.e., ≤ 0.25 [16,28] (see Table 1 and captions of relevant figures). The bond length parameters $\sigma_{\alpha\beta}$ remain unchanged for the tip-slider interactions. An external force is applied in the y-direction on the slider to control the normal stress. For all sliding simulations presented, the external normal force is kept constant such that the contact stress (normalized by a nominal contact area) is constant. Following our previous study[16,28], this nominal contact area is taken as the cross-section area of the intact tip, ignoring the tip elastic deformation and possible material build-up at the trailing end of the tip. With atomic smoothness, an intimate contact forms immediately between the slider and the tip [16]. We note that although in a linear-elastic continuum analysis [34] there exists a stress singularity at the edge of the tip, we do not observe singularity at the atomic scale in both the normal and shear stress using stress analysis based on the interatomic force between the slider atoms and the tip atoms at different contact areas in our simulations [28]. The reasons include (1) the breakdown of continuum models [8], (2) the different definitions of stress adopted at different scales [35–38], and (2) build-up of local stress would increase the wear locally which limits any further increase of the local stress.

The slider moves at a constant sliding speed in the x-direction as shown in Fig. 1 A. A constant wear rate is reached quickly (run-in process can be ignored) [16] and no fracture-induced debris [22] is generated. The wear rate is measured by dH/dL in terms of slider height (H) reduction per sliding distance dL, which is equivalent to the volume change per sliding distance $dV/dL = AdH/dL$ with a constant contact area A. Example curves of the slider height H at different time are given in Fig. 1B. In all sliding simulations, a highly linear relation is found between the height of the slider and the sliding distance. Therefore, the

wear rate in the slider-tip system is expressed as the decreasing height of the tip per unit sliding distance dH/dL. This is particularly useful for a constant contact area wear simulations. These wear rate measurements have been used in previous studies [10,16,18]. The wear curves are insensitive to the tip height according to sliding simulations using a tip twice higher (not shown). The total sliding distance was adjusted according to the sliding velocity to make sure at least two layers of atoms are removed. The only exception is for the slowest velocity (0.012 m/s) where we have simulated only up to 3 μm seconds.

2.3. Measurement of T_{eff} of the atomic wear

The slider-tip system is a typical non-equilibrium system where mechanical energy is supplied continuously and dissipated into heat. Instead of conventional thermal activation for wear, we propose a mechanical, athermal activation mechanism (see following sections). For athermal activation in steady-state non-equilibrium systems (where one can still define and calculate $T_{kinetic}$ using $\frac{3}{2}k_B T_{kinetic} = \frac{1}{2} < mv^2 >$), the effective temperature T_{eff} plays the role of thermodynamic temperature in equilibrium systems that characterizes the degree to which non-equilibrium systems sample phase space in the presence of an external field.

Measurements of T_{eff} have been performed in non-equilibrium systems [39–41], such as colloidal glasses, granular materials, and foams, but T_{eff} has not been measured in slider-tip systems that give rise to wear. Most previous measurements of T_{eff} have been carried in bulk systems. In contrast, the interface in slider-tip systems where atomic wear occurs is confined as thin as one to two layers of atoms, and T_{eff} varies strongly with the surface depth. In equilibrium systems, there are several equivalent definitions of temperature. In out-of-equilibrium systems, however, these definitions are not necessarily equivalent. Two methods to measure T_{eff} were attempted in this study: (I) a fluctuation-dissipation relation for the wave-number dependent density [39–41] and (II) the equipartition theorem for the translational degrees of freedom of a massive tracer particle [42,43]. The tribo-system setup used for T_{eff} measurement is illustrated in Fig. 1 C where periodic boundary conditions are applied in the plane of contact. The setup is similar to Fig. 1 A except that both the tip and the slider are continuous. This enables calculations for both the density autocorrelation function and response function for the tip atoms on the top without complication from loss of particles.

In method (I), the integrated response $R_{\rho(k)}$ of the large particle number density at wave vector in the z-direction is plotted against the density autocorrelation function $C_{\rho(k)}$ at the same wave vector. The definitions of $R_{\rho(k)}$ and $C_{\rho(k)}$ are given by Ref. [39]:

$$R_{\rho(k)}(t) = \frac{\langle O(t) - O(0) \rangle}{h_O}, \tag{4}$$

where h_O is a constant field that is conjugate to the observable

$$O(t) = \frac{1}{N_L} \sum_{j=1}^{N_L} \varepsilon_j \exp\left[i \vec{k} \cdot \vec{r}_j(t) \right], \tag{5}$$

where N_L is the number of the large particles, $\varepsilon_j = \pm 1$ is a bimodal random variable with 0 mean and is the position of the jth atom at time t. With this choice of observables, the correlation function is essentially the incoherent part of the intermediate scattering function for the large particles:

$$C_{\rho(k)}(t) = \frac{1}{N_L} \sum_{j=1}^{N_L} \left\langle \exp\left\{ i \vec{k} \cdot \left[\vec{r}_j(t + t_0) - \vec{r}_j(t_0) \right] \right\} \right\rangle. \tag{6}$$

Both $R_{\rho(k)}$ and $C_{\rho(k)}$ are calculated using particle positions of atoms within 0.6 nm of the tip. A thickness of 0.6 nm is used here because it is the first layer of atoms in the tip that mainly contributes to atomic wear [44]. Moreover, we found a thicker surface layer results in a similar T_{eff} (not shown).

In method (II), T_{eff} is measured using a special thermometer that has the same characteristic time scale associated with T_{eff}. A heavy tracer particle of mass m_{tr} serves as such a thermometer, as its Einstein frequency is closer to that of the mechanical agitation [42,43]. From the generalized equipartition theorem, one can calculate the average kinetic energy to estimate the effective temperature using. Note that the tracer particle velocity along the z-direction transverse to the sliding direction is used [42,43]. The tracer particles were chosen from the existing tip atoms and assigned with new masses.

2.4. Simplified wear simulations using Generalized Langevin Dynamics (GLD)

To investigate the role T_{eff} plays in atomic wear, we conducted wear simulations using a toy model by coupling a thin layer of atoms with a generalized Langevin dynamics thermostat, see Fig. 1D. The tip is a binary Lennard-Jones glass using the same Wahnstrom parameters. The bottom layer (~0.6 nm) of the sample is held rigid. A constant normal stress along the y-direction is applied on the tip material by a perfect flat wall interacting with the tip with a Lennard-Jones 9–3 potential:

$$\phi_w = \varepsilon_w \left[\frac{2}{15} \left(\frac{\sigma_w}{y_w - y} \right)^9 - \left(\frac{\sigma_w}{y_w - y} \right)^3 \right]. \tag{7}$$

ε_w represents the bonding energy between tip atoms and the wall and σ_w provides a length scale (the distance at which the interaction energy is zero). y_w-y is the distance from the wall to the atom. ε_w, σ_w and the potential cutoff are set to be $0.2\varepsilon_{LL}$, σ_{LL} and $2.5\sigma_{LL}$, respectively. Thus, in this setup, we only consider the motion of a confined layer between the rigid substrate and a frictionless wall. This confined layer is $\sim 2\sigma_{LL}$ in thickness, consistent with the observation in the sliding simulations that the atomic wear is mainly confined to the top layer of the tip.

Because the flat wall is frictionless, shear stress is applied to the tip material by superimposing a constant lateral force f in the x-direction. PBC is applied in the x-z plane so that tip atoms will not be lost or worn off. Consequently, the effects of the tip edge and debris accumulation in the trailing end are not considered. The agitation from the roughness of the slider on the tip atoms is modeled by applying a GLD thermostat set at T_{eff} coupled with the middle layer. Thus, this layer is coupled to two temperature baths: (1) a Langevin thermostat at $T_{kinetic}$ and (2) a generalized Langevin dynamics thermostat at T_{eff}. A similar setup has been used previously to study activation dynamics [45,46]. The two thermal baths give the equation of motion:

$$m\dot{v} = -V'(x) - \int_0^t ds \Gamma(t-s) v(s) - \Gamma_0 v(t) + \xi(t) + \eta(t). \tag{8}$$

Γ_0 and η(t) are the frictional drag and random noise strength, respectively, for the Langevin thermostat, where $\langle \eta(t)\eta(s) \rangle = 2T_{bath}\delta(t - s)$. $\Gamma(t\text{-}s)$ and $\xi(t)$ are the frictional drag and random noise strength for the GLD thermostat, where $\langle \xi(t)\xi(s) \rangle = 2T_{eff}\Gamma(t - s)$. For the memory kernel, we use a Prony form:

$$\Gamma(t) = \frac{c_k}{\tau_k} e^{-t/\tau_k}, \tag{9}$$

where τ_k is the time constant. Here we let $c_k = \tau_k$ following Ref. [46]. It has been found [46] that for the conditions $\tau_k >> 1$ or $c_k/\tau_k >> 1$, there will be a separation of time scales associated with T_{eff} and $T_{kinetic}$ [21]. Eq. 9 enables the mapping of the non-Markovian dynamics (Eq. 8) onto a Markovian problem [45].

As we are simulating the motion of top layer atoms in the tip with a periodic boundary setup in the GLD simulations, a conversion from the displacement of these atoms to the wear rate is needed, assuming debris formation comes from the mass flow with a constant flow speed of the top layer of the tip material. One can define the average flow velocity of

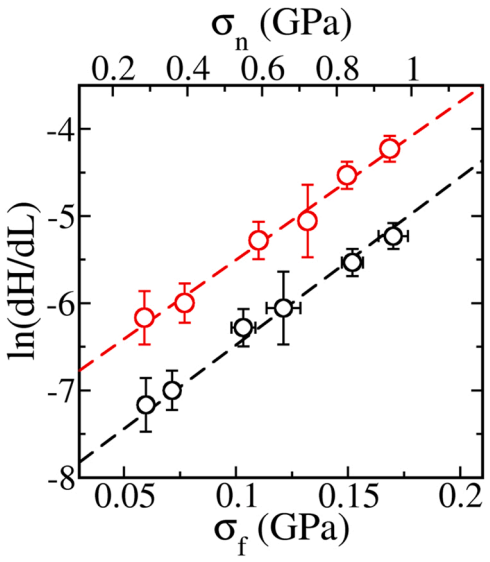

Fig. 2. Variation of the wear rate with shear stress σ_f (black) and normal stress σ_n (red) ($T_{kinetic}$ =63 K, $\kappa = 0.10$, v_0≈12 m/s) for a rectangular tip of 6 nm long. The normal stress data are shifted vertically for clarity. A linear fit gives slope $V_{act}/k_BT = 17.7 \pm 0.6$ GPa^{-1} and 3.0 ± 0.2 GPa^{-1} for σ_f and σ_n, respectively.

the top layer as$\bar{v} = \frac{\sum_{i=1}^{N} \Delta x_i}{N \cdot \Delta t}$. Here Δx_i *is* the atomic displacement relative to the initial position and N is the number of atoms in the top layer. $N = \frac{l_x l_z h_{top}}{v_m}$, l_x and l_z are the tip lengths in the x- and z-directions, h_{top} is the thickness of the top layer, and v_m is the molecular volume. Therefore, the debris volume is $\Delta V = \bar{v} \cdot \Delta t \cdot l_z \cdot h_{top}$ and the tip height loss during the time period Δt can be written as

$$\Delta H = \frac{\sum_{i=1}^{N} \Delta x_i}{l_x} \cdot \frac{v_m}{l_x \cdot l_z}. \tag{10}$$

The GLD parameter τ_k characterizes the typical time scale for athermal activation. Therefore, for a simulation duration of time t, there are t/τ_k activation events from sliding. The corresponding sliding distance in a tip-wear MD simulation would be

$$\Delta L = t/\tau_k l_r \tag{11}$$

l_r is the characteristic length scale for the slider surface roughness, which was chosen to be the atomic radius of 0.27 *nm* for simplicity. It should be noted that the atomic wear behavior is independent of the choice of τ_k, which is analogous to the fact that the atomic wear rate is insensitive to the sliding speed. Fig. A.1 in Appendix A shows that the wear rate is weekly dependent on the τ_k. A reasonable value of τ_k can be estimated using the tip wear MD simulations (Section 2.2). For an MD simulation with a sliding speed of 12 *m/s*, and an atomic roughness on the order of the atomic radius 0.27 *nm*, the time between two mechanical activation events is ~25 *ps*. This situation corresponds to a τ_k of 25 *ps*. Thus, τ_k = 25 *ps* is used in the GLD simulations.

The advantages of the GLD simulations are that T_{eff} can be controlled independently from $T_{kinetic}$, and the shear stress can be controlled independently from the normal stress. Although simplified, the GLD simulations can reproduce key features of the atomic wear MD simulations.

3. Results and discussion

3.1. Atomic wear in Lennard-Jones system

Starting with the sliding simulation for atomic wear, the dependence of the wear rate on the contact stress is shown in Fig. 2. *dH/dL* is an

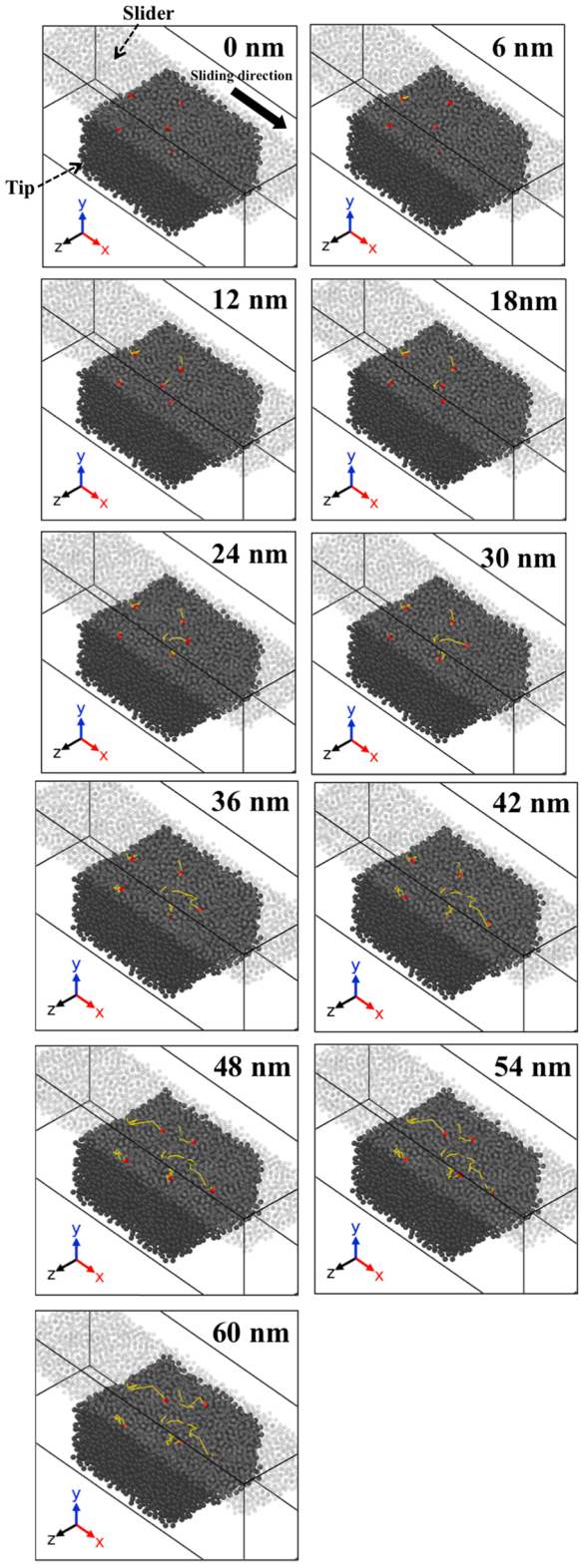

Fig. 3. A series of snapshots from the atomic wear simulation. The wear parameters are: $T_{kinetic}$ = 63 K, $\kappa = 0.1$, σ_n≈ 0.4 GPa, v_0≈ 12 m/s. The sample is 6 nm long in x-direction. The sliding distance of each snapshot is shown on the top-right corner of each panel. We have made the slider semi-transparent and selected five tip debris atoms (red and ignoring their types) which are moving during the sliding to trace their trajectories (yellow lines).

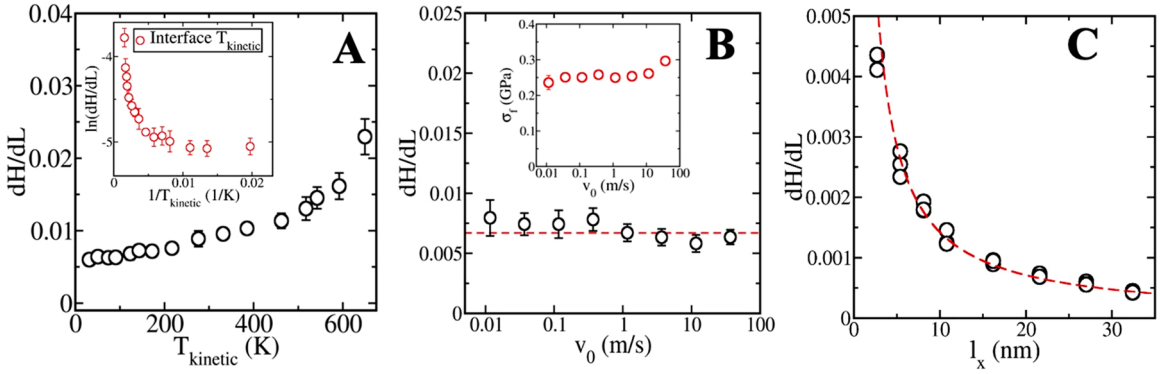

Fig. 4. Variation of the wear rate with (A) $T_{kinetic}$ ($\kappa = 0.25$, $\sigma_n \approx 0.1$ GPa, $v_0 \approx 12$ m/s), (B) sliding speed v_0 ($\kappa = 0.25$, $T_{kinetic} = 63$ K, $\sigma_n \approx 0.1$ GPa) and (C) tip length l_x ($\kappa = 0.2$, $\sigma_n \approx 0.2$ GPa, $v_0 \approx 12$ m/s). The inset of (A) shows the semi-log plot of the same data as a function of $1/T_{kinetic}$. The inset of (B) shows that the shear stress σ_f remain nearly unchanged. The non-linear fit in (C) uses data from three different samples and assumes $dH/dL = c/l_x$. The fitted curve has a correlation coefficient of 0.99 with $c = 0.014$ nm. Error bars reported for (A) and (B) are estimated from standard deviation of five and three parallel samples, respectively. Note error bars smaller than the symbol size are not shown.

exponential function of the normal stress (σ_n) and frictional shear stress (σ_f), a hallmark of the atomic wear regime as reported in Refs. [4,5,9,10,11,13,14,28]. The atomic wear observed in the Lennard-Jones system consists of intermittent motion by a small fraction of the top layer tip atoms adjacent to the slider. A series of snapshots from the atomic wear simulation (sliding conditions: $T_{kinetic} = 63$ K, $\kappa = 0.1$, $\sigma_n \approx 0.4$ GPa, $v_0 \approx 12$ m/s) are shown in Fig. 3 (note the displacement of these atoms is much smaller than the sliding distance L). This is very different from shear banding where all atoms inside the shear band participate the deformation [47]. Next we show how the wear rate in the atomic wear regime varies as a function of temperature, sliding speed, and contact area.

3.2. Effect of temperature and sliding speed on atomic wear

Fig. 4A shows the variation of the wear rate dH/dL with the bath temperature $T_{kinetic}$ ($T_{kinetic}$ is calculated using $\frac{3}{2}k_B T_{kinetic} = \frac{1}{2} < mv^2 >$ where the right is the average kinetic energy). The non-exponential dependence of dH/dL on $T_{kinetic}$ can be further seen from the Arrhenius-type plot in the inset of Fig. 4 A. In our simulations, we have used $T_{kinetic}$ measured from tip atoms at the interface as it is slightly higher than the thermostat by 15 K or less. Fig. 4B shows the sliding velocity (v_0) dependence of atomic wear. The wear rate is nearly constant for v_0 spanning almost four orders of magnitude as indicated by the red horizontal line (at least two layers of atoms were removed in these simulations). $T_{kinetic}$ only varies from 63 K to 74 K over this range of v_0, which has a minor effect according to Fig. 4 A. As v_0 increases beyond 30 m/s, the wear rate increases dramatically due to significant frictional heat. According to thermally-activated friction models [48–50], the shear stress increases logarithmically or sub-logarithmically with the sliding velocity before it reaches a critical value and becomes velocity-independent beyond the critical velocity [20,21,49]. Because much higher velocities (>10 mm/s) were used in our simulations than those in the literatures [20,49] (<10 μm/s), σ_f remains unchanged at 0.26 ± 0.02 GPa as shown in the inset of Fig. 4B. The temperature and sliding velocity dependences suggest that the atomic sliding for the Lennard-Jones glass model is an *athermal* activation process as opposed to an Eyring-like activation process for the range of v_0 investigated.

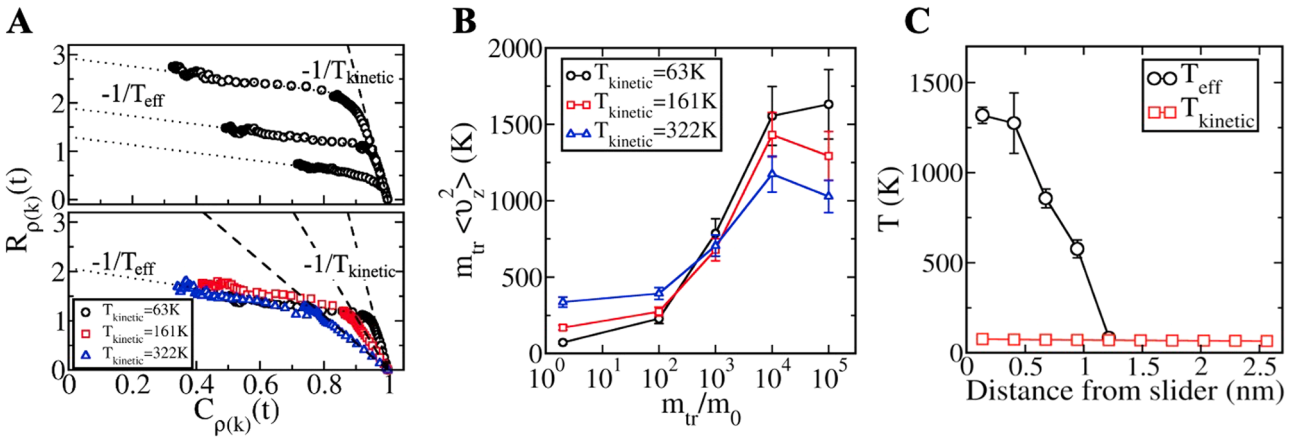

Fig. 5. Two methods are employed to measure T_{eff} (The contact stress σ_n is 0.05 GPa, adhesion strength $\kappa = 0.25$, and sliding speed $v_0 \approx 12$ m/s.): (A) $R_{\rho(k)}$ vs $C_{\rho(k)}$ of the interface atoms in the slider-tip wear system. $T_{kinetic} = 63$ K for the top panel. The wave vectoris in the z-direction transverse to the sliding direction. In the top panel, we show $R(C)$ curves for $=k\hat{z}$ for three wavenumbers k = 11.5, 7.67 and 3.83 (from top to bottom). The dotted lines are guides to the eye showing that the $R(C)$ curves for different wavenumbers give similar values for T_{eff} (1500 K~2050 K), which corresponds to the inverse slopes of the curves at long times. The dashed line shows the initial slope, $-1/T_{kinetic}$. The bottom panel shows $R(C)$ curves at three values for $T_{kinetic}$. The dotted line shows that T_{eff} does not change significantly for the three values of $T_{kinetic}$ which is given by the dashed lines. (B) T_{eff} measured using the heavy tracer method as a function of the mass of the tracer particle for several values of $T_{kinetic}$. The error bars are evaluated from standard deviation of multiple samples. (C) T_{eff} and $T_{kinetic}$ as a function of the distance from the center of the slider ($\kappa = 0.25$, $\sigma_n \approx 0.1$ GPa, $v_0 \approx 12$ m/s). T_{eff} was measured using fluctuation-dissipation relations and each point in the plot corresponds to the T_{eff} of a thin layer of ~0.3 nm. The error bar for T_{eff} is estimated from standard deviation of three larger samples (Table 1). The error bar for $T_{kinetic}$ is smaller than the symbol size.

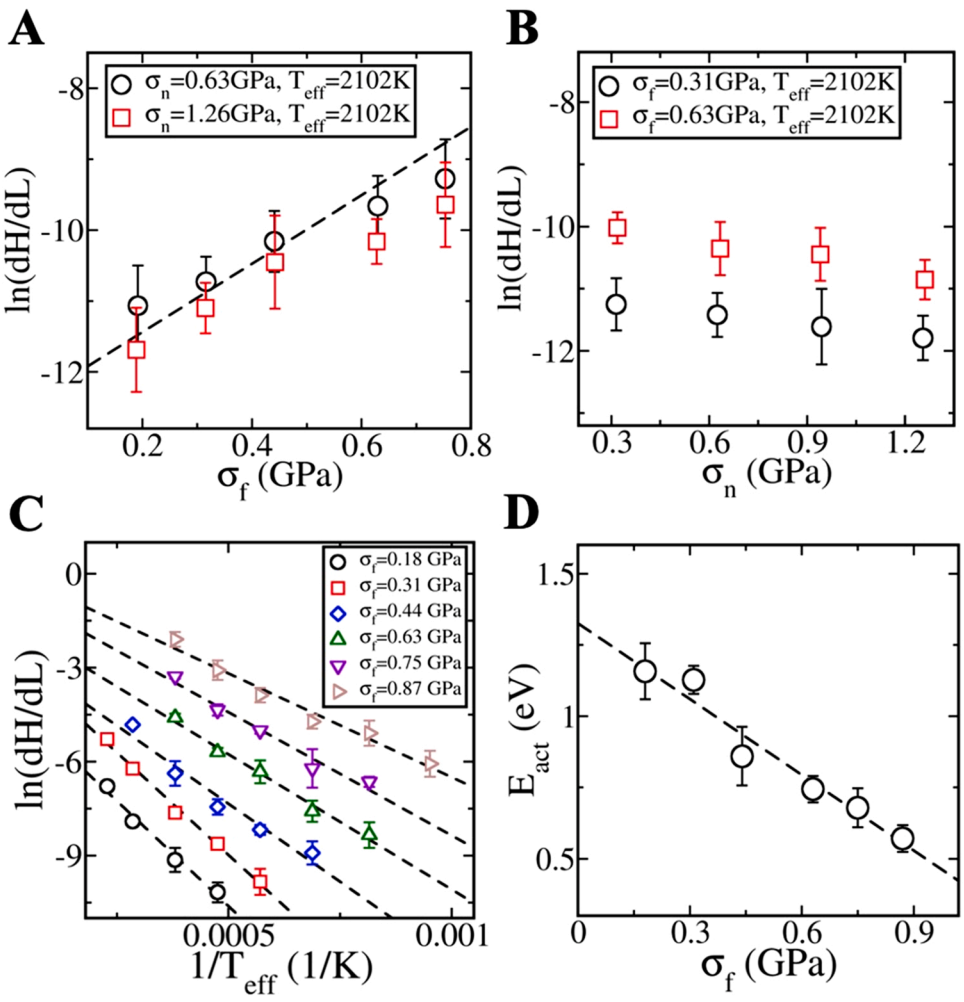

Fig. 6. Variation of the wear rate *ln (dH/dL)* with (A) shear stress σ_f, (B) normal stress σ_n, and (C) T_{eff}. In (A) and (B), $T_{kinetic}$= 63 K. In (C), σ_n= 0.3 GPa and $T_{kinetic}$= 63 K are used in the GLD simulations. The lowest shear stress, 0.18 GPa, has the correct scale and all other data are shifted for clarity. (D) The activation energy E_{act} extracted from (C) is plotted against σ_f. The dashed line in (A) has the slope V_{act} obtained in (D). A sliding speed v_0 of 12 m/s was assumed to calculate *dH/dL*. The error bars are from standard deviation of five independent samples.

3.3. Sample size effect on atomic wear

Next, we examined how the contact area affects the wear rate in the atomic wear regime, which has not been considered in the literature [4,9,10] as bond breaking events are directly used to calculate the wear rate. Based on this notion, atomic wear rate *dH/dL* would be independent of contact area and the tip length l_x in the sliding direction under otherwise identical sliding conditions. However, Fig. 4 C shows that the wear rate in the Lennard-Jones glass system is inversely proportional to l_x at the same contact stress. The sliding conditions are $\kappa = 0.2$, $\sigma_n \approx 0.2$ GPa and $v_0 \approx 12$ m/s respectively. Therefore, bond breaking does not directly lead to debris-generation, i.e. debris atoms form only when they leave the interface at the edge of the contact (see Fig. 3). This is a crucial point for formulating an effective atomic wear equation for the Lennard-Jones glass as will be discussed later.

3.4. Effective temperature in the tribo-system

Based on the above MD results from the Lennard-Jones glass model for which existing wear formula is not applicable, we propose a mechanical activation mechanism for the atomic wear by adopting the effective temperature T_{eff}, a concept playing the role of thermodynamics temperature in equilibrium system for a non-equilibrium system. Different definitions of T_{eff} have been proposed in non-equilibrium systems such as granular materials [40,51,52]. However, T_{eff} has been rarely measured in any tip wear tribo-systems. Two methods were applied to measure T_{eff} (see Section 2.3): (I) fluctuation-dissipation relations of the number density and (II) equipartition for the translational degrees of freedom using massier particles.

Using method (I), Fig. 5 A shows the integrated response $R_{\rho(k)}$ of the large particle number density at wave vector in the z-direction transverse to the sliding direction versus the density autocorrelation function $C_{\rho(k)}$ at the same wave vector. The sliding conditions are $\sigma_n \approx 0.05$ GPa, $\kappa = 0.25$, and $v_0 \approx 12$ m/s, respectively. These *R(C)* curves have two characteristic regimes as predicted by Kurchan [51], similar to observations made in studies of sheared Lennard-Jones glasses [42]. At short times, the slope of the *R(C)* curves, $-1/T_{kinetic}$, is determined by the thermostat temperature, and corresponds to fast relaxations. At long times, the slope of the *R(C)* curves, $-1/T_{eff}$, corresponds to relaxations that occur from shearing at the tip-slider interface. The curves and the parallel dotted lines shown in the upper panel of Fig. 5 A give T_{eff} ~1790 K for three different wave vectors, which is consistent with previous results. The lower panel of Fig. 5 A shows that the slope at small *R* and *C* (~1) varies with $T_{kinetic}$ (see the dashed lines) while T_{eff} is nearly constant when $T_{kinetic}$ changes from 63 K to 322 K. Overall, the obtained $T_{eff} = 1500$–2050 *K* is much higher than $T_{kinetic}$ (60–350 *K*).

With the same sliding conditions, we have measured T_{eff} using tracer particles, i.e., method (II). The results are shown in Fig. 5B. Each data

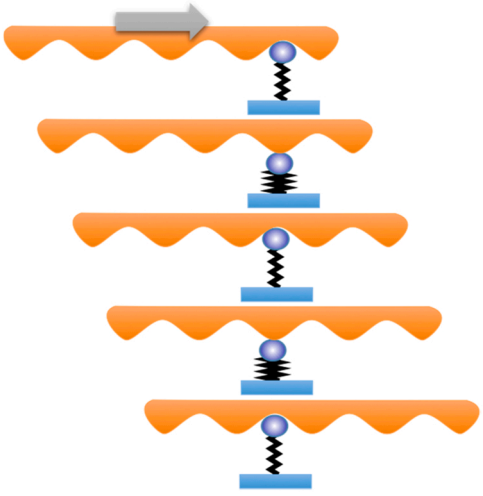

Fig. 7. A schematic for the mechanically-activated atomic wear picture, showing the consecutive agitation of the slider to the blue atom and the number of such agitation is proportional to the sliding distance.

point represents an average of at least ten simulations with different tracer particles. Light particles (m_{tr}~10^0 –10^2 m_0) give the temperature of the fast thermostat, i.e. $T_{kinetic}$. The effective temperature crosses over to above 1000 K, i.e. T_{eff} for heavier particles (m_{tr}~10^4 –10^5 m_0). These results are similar to those reported by Berthier and Barrat in sheared Lennard-Jones glasses [42,43]. In Fig. 5B we show that the effective temperatures at different $T_{kinetic}$ are close to each other, in agreement with the results from Fig. 5 A. The T_{eff} (1180–1560 K) measured from tracer particles is close to the T_{eff} (1500 K~2050 K) measured from *R(C)* curves. Differences between the two measured effective temperature may exist due to the following reasons: (1) the extremely heavy particles may affect the slider-tip interactions and (2) T_{eff} obtained from the *R(C)* plot is averaged over all atoms within a certain depth (0.6 nm), while the T_{eff} from the tracer particle measurement corresponds to the outmost layer of the tip.

Because only those tip atoms close to the slider are undergoing mechanical agitation from the slider, the effective temperature will be different for tip atoms at different depths. Fig. 4 shows that T_{eff} drops quickly away from the interface and becomes equal to $T_{kinetic}$ at distances > 1.2 nm from the slider. The sliding conditions are $\kappa = 0.25$, $\sigma_n \approx 0.1$ GPa, and $v_0 \approx 12$ m/s, respectively.

3.5. Wear simulations using generalized Langevin dynamics

To illustrate that atomic wear can be activated athermally in an Arrhenius plot, one needs a series of atomic wear simulations with identical contact stress states over a range of effective temperatures. However, T_{eff} varies in a relatively narrow range in our tip wear simulations. To overcome this, we conduct GLD simulations of the top layer of the tip atoms (see Section 2.4). In these slider-free simulations, the tip atoms are coupled to two heat baths at two concepts of temperature: a fast bath held at $T_{kinetic}$ and a slow bath held at T_{eff} with $T_{eff} \gg T_{kinetic}$ (T_{eff} represents the mechanical agitation from the slider to the tip atoms).

Fig. 6 A shows that the wear rate in the GLD simulations (calculated from atomic flux in the sliding direction; see Section 2.4) increases exponentially with the shear stress, whereas it is insensitive to the normal stress with only a slight decrease as shown in Fig. 6B. Therefore, the shear stress, not the normal stress, induces mechanical agitation for atomic wear. Fig. 6 C shows the wear rate versus T_{eff} in an Arrhenius-type plot for various shear stress σ_f with the normal stress and $T_{kinetic}$ unchanged. It is clear that T_{eff} is able to capture the mechanical activation of debris generation. The activation energy E_{act} can be determined from the slope of $\ln(dH/dL)$ versus $1/T_{eff}$ in Fig. 6 C at different values of σ_f. As σ_f increases, E_{act} decreases as shown in Fig. 6D. Extrapolation of E_{act} to $\sigma_f = 0$ gives the stress-free activation energy E_0 of 1.33 ± 0.06 eV, which is the same order of magnitude as the cohesive energy (1.0 eV/atom) of the Lennard-Jones system. The slope of E_{act}–σ_f curve gives an activation volume V_{act} of 0.14 ± 0.02 nm^3. The value corresponds to the volume of one or two atoms, which is consistent with the atom-by-atom attrition picture. For the MD simulation results shown in Fig. 2, together with the measured T_{eff}, the athermal activation volume is estimated to be 0.26–0.42 nm^3. Prior experiments [4,9–11,17] reported values of V_{act} over a wide range from an order of 0.001–0.1 nm^3. The large difference in V_{act} between our simulations and experimental results comes firstly from the use of T_{eff} instead of $T_{kinetic}$. Another difference is that V_{act} in this work is conjugate to shear stress (as validated in Fig. 5B), while some V_{act} in prior experiments are conjugate to normal stress [4,9,10] or radial stress [11]. Lastly, our MD simulations (Fig. 2) were conducted at much higher sliding velocities whereas much lower velocities are typically applied in experiments except those using a polymer substrate [5,10,53].

3.6. A wear formula for the Lennard-Jones system

We now attempt to develop a wear formula for the Lennard-Jones glass system which is athermally activated, shear-facilitated, and tip-size dependent. A schematic picture is shown in Fig. 7. The tip atom (blue) is mechanically agitated by the surface corrugation of the slider. Such mechanical agitation facilitates the rearrangement of tip-surface atoms which is characterized by T_{eff} and can occur even at a low $T_{kinetic}$. The mechanical agitation of a moving slider is not strongly dependent on its speed: both the shear stress (as shown in the inset of Fig. 4B) and T_{eff} are roughly independent of the sliding speed. The number of agitation attempts per atom can be approximated as the sliding distance divided by a characteristic length scale for roughness l_r. In other words, the sliding distance in athermal activation plays the role of time in thermal activation. An immediate consequence is that the wear rate becomes independent of the sliding velocity, which agrees with our MD simulation results. In addition, Fig. 4 C shows that the atomic wear rate $dH/dL \propto 1/l_x$ or $dV/dL \propto l_z$ (l_z is the thickness of the tip). We rationalize this observation by recognizing that the atomic wear process consists of discrete atomic jumps: only debris events within a certain distance (an average jumping distance l_j) to the edge of the tip can reach the edge of the tip thus contribute to the wear rate; while atomic movement deep inside the tip constitute a continuous stream of atoms not yet reaching the edge of the tip. Alternatively, if the debris events of the entire contact contribute to the overall wear rate, then $dV/dL \propto l_x l_z$, contradicting to Fig. 4 C.

From the above discussions, the actual area contributing to debris formation for the rectangular tip is the product of the tip thickness l_z and the average jumping distance l_j. For a cylindrical tip, the area will be the product of the diameter of the tip 2 *R* and the average jumping distance l_j. Thus, the total number of attempts $N_{attempt}$, based on mechanical agitation, can be written as,

$$N_{attempt} = l_z l_j n_s \frac{L}{l_r}, \tag{12}$$

where n_s is the areal number density for tip atoms and l_r is the characteristic length for slider roughness. l_z l_j n_s is the number of atoms within the effective area near the tip edge. These atoms, once they make a movement toward the sliding direction, can escape the contact area. L/l_r is the number of mechanical agitations for each surface atom due to sliding. According to Eq. (1), with T_{eff} substituting $T_{kinetic}$, the wear rate

of worn volume per sliding distance can be written as

$$\frac{dV_{debris}}{dL} = l_z \cdot b \cdot \exp\left(-\frac{E_a - \sigma_f V_{act}}{k_B T_{eff}}\right), \quad (13)$$

where $b = \frac{l_j n_s v_m}{l_r}$ has a unit of length wherein v_m is the molecular volume. Because the contact area is $l_x l_z$, the height loss per sliding distance can be expressed as

$$\frac{dH}{dL} = \frac{b}{l_x} \cdot \exp\left(-\frac{E_a - \sigma_f V_{act}}{k_B T_{eff}}\right), \quad (14)$$

which is consistent with the results in Fig. 4 C. Alternatively, for a tip with circular contact with radius R, the number of atoms within the effective area near the tip edge is $2Rl_j n_s$ and the contact area is πR^2. Following the same steps as above, the wear rate can be expressed as,

$\frac{dV}{dL} = R \cdot b \cdot \exp\left(-\frac{E_a - \sigma_f V_{act}}{k_B T_{eff}}\right)$ or $\frac{dH}{dL} = \frac{b}{\pi R} \cdot \exp\left(-\frac{E_a - \sigma_f V_{act}}{k_B T_{eff}}\right)$ (15).

4. Conclusions

In summary, we used molecular scale simulations to investigate tip wear of a Lennard-Jones model glass in the atomic wear regime over a range of temperatures, sliding velocities, and contact radii. The wear results are inconsistent with the atomic wear models based on thermal activation without debris re-deposition. We thus propose an effective formulation for atomic wear observed in the model glassy tribosystem that is athermally activated, facilitated by shear stress, and tip-size dependent. This wear formulation suggests that the thermal activation mechanism using the conventional concept of temperature is not universally applicable in all types of atomistic wear such as the one we observed in the simple Lennard-Jones model at relatively high sliding velocities. In this regard, this work has provided some critical factors to include in order to improve quantitative assessment of the service lifetime of nanoscale devices particularly under low contact stresses and high sliding speeds. Extension of our work to materials such as those with covalent bonds will further shed light on the wear behavior in more complicated systems.

Declaration of Competing Interest

The authors declare that they have no known competing financial interests or personal relationships that could have appeared to influence the work reported in this paper.

Data Availability

The data that support the findings of this study are available from the corresponding author upon reasonable request.

Acknowledgements

We thank Professors Thierry Blanchet (Rensselaer Polytechnic Institute), Izabela Szlufarska (University of Wisconsin), Robert Carpick (University of Pennsylvania), Mark Robbins (Johns Hopkins University), and Michael Falk (Johns Hopkins University) for useful discussions. We are grateful for support from the National Science Foundation under Grant No. CMMI-1031408. Molecular dynamics simulations were carried out in LAMMPS using supercomputers in the Computational Center for Innovations (CCI) at RPI.

Appendix A. Effect of τ_k on wear rate in GLD simulations

(see Fig. A1)

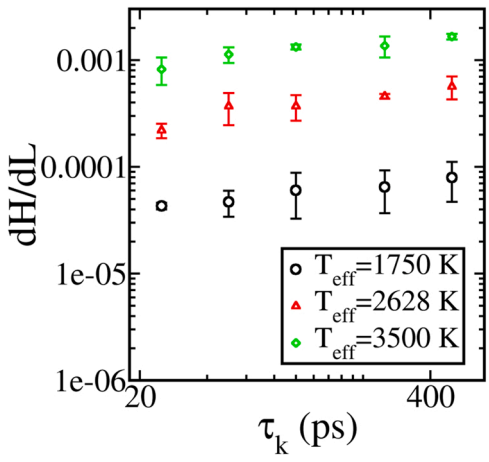

Fig. A1. Log-log plot of dH/dL versus τ_k at different T_{eff} measured in the GLD simulations. The atomic wear rate remains nearly constant as τ_k is varied from 25 to 500 *ps*. The normal stress and shear stress are 0.31 GPa and 0.63 GPa, respectively. The error bars are estimated from standard deviation of three samples.

References

[1] Archard JF. Contact and Rubbing of Flat Surfaces. J Appl Phys 1953;24:981–8. https://doi.org/10.1063/1.1721448.
[2] Rajauria S, Canchi SV, Schreck E, Marchon B. Nanoscale wear and kinetic friction between atomically smooth surfaces sliding at high speeds. Appl Phys Lett 2015; 106. https://doi.org/10.1063/1.4913465.
[3] Rajauria S, Schreck E, Marchon B. Voltage assisted asymmetric nanoscale wear on ultra-smooth diamond like carbon thin films at high sliding speeds. Sci Rep 2016;6.
[4] Bhaskaran H, Gotsmann B, Sebastian A, Drechsler U, Lantz MA, Despont M, et al. Ultralow nanoscale wear through atom-by-atom attrition in silicon-containing diamond-like carbon. Nat Nanotechnol 2010;5:181–5. https://doi.org/10.1038/nnano.2010.3.
[5] Lantz MA, Wiesmann D, Gotsmann B. Dynamic superlubricity and the elimination of wear on the nanoscale. Nat Nanotechnol 2009;4:586–91. https://doi.org/10.1038/nnano.2009.199.
[6] Szlufarska I, Chandross M, Carpick RW. Recent advances in single-asperity nanotribology. J Phys Appl Phys 2008;41:123001. https://doi.org/10.1088/0022-3727/41/12/123001.
[7] Mate CMathew. Tribology on the small scale. Oxford: Oxford University Press; 2008.
[8] Luan B, Robbins MO. The breakdown of continuum models for mechanical contacts. Nature 2005;435:929–32. https://doi.org/10.1038/nature03700.
[9] Jacobs TDB, Carpick RW. Nanoscale wear as a stress-assisted chemical reaction. Nat Nanotechnol 2013;8:108–12. https://doi.org/10.1038/nnano.2012.255.
[10] Gotsmann B, Lantz MA. Atomistic wear in a single asperity sliding contact. Phys Rev Lett 2008;101:125501. https://doi.org/10.1103/PhysRevLett.101.125501.
[11] Park N-S, Kim M-W, Langford SC, Dickinson JT. Atomic layer wear of single-crystal calcite in aqueous solution using scanning force microscopy. J Appl Phys 1996;80:2680.
[12] Sheehan PE. The wear kinetics of NaCl under dry nitrogen and at low humidities. Chem Phys Lett 2005;410:151–5. https://doi.org/10.1016/j.cplett.2005.05.060.
[13] Jacobs TDB, Gotsmann B, Lantz MA, Carpick RW. On the application of transition state theory to atomic-scale wear. Tribol Lett 2010;39:257–71. https://doi.org/10.1007/s11249-010-9635-z.
[14] Shao Y, Jacobs TDB, Jiang Y, Turner KT, Carpick RW, Falk ML. Multibond model of single-asperity tribochemical wear at the nanoscale. ACS Appl Mater Interfaces 2017;9:35333–40. https://doi.org/10.1021/acsami.7b08023.
[15] Wang W, Dietzel D, Schirmeisen A. Thermal activation of nanoscale wear. Phys Rev Lett 2021;126:196101. https://doi.org/10.1103/PhysRevLett.126.196101.
[16] Yang Y, Huang L, Shi Y. Adhesion suppresses atomic wear in single-asperity sliding. Wear 2016;352:31–41.
[17] Martini A, Kim SH. Activation volume in shear-driven chemical reactions. Tribol Lett 2021;69:150. https://doi.org/10.1007/s11249-021-01522-x.
[18] Vargonen M, Yang Y, Huang L, Shi Y. Molecular simulation of tip wear in a single asperity sliding contact. Wear 2013;307:150–4. https://doi.org/10.1016/j.wear.2013.09.004.
[19] Sha Z-D, Sorkin V, Branicio PS, Pei Q-X, Zhang Y-W, Srolovitz DJ. Large-scale molecular dynamics simulations of wear in diamond-like carbon at the nanoscale. Appl Phys Lett 2013;103:073118. https://doi.org/10.1063/1.4818713.
[20] Li Q, Dong Y, Perez D, Martini A, Carpick RW. Speed dependence of atomic stick-slip friction in optimally matched experiments and molecular dynamics simulations. Phys Rev Lett 2011;106:126101.
[21] Dong Y, Li Q, Martini A. Molecular dynamics simulation of atomic friction: a review and guide. J Vac Sci Technol A 2013;31:030801. https://doi.org/10.1116/1.4794357.

[22] Aghababaei R, Warner DH, Molinari J-F. Critical length scale controls adhesive wear mechanisms. Nat Commun 2016;7:11816. https://doi.org/10.1038/ncomms11816.
[23] M.O. Robbins, M.H. Müser, Computer simulations of friction, lubrication and wear, ArXiv Prepr. Cond-Mat0001056. (2000). http://arxiv.org/abs/cond-mat/0001056 (Accessed 2 September 2016).
[24] Maloney CE, Robbins MO. Evolution of displacements and strains in sheared amorphous solids. J Phys Condens Matter 2008;20:244128. https://doi.org/10.1088/0953-8984/20/24/244128.
[25] Pastewka L, Moser S, Gumbsch P, Moseler M. Anisotropic mechanical amorphization drives wear in diamond. Nat Mater 2011;10:34–8. https://doi.org/10.1038/nmat2902.
[26] Pastewka L, Pou P, Pérez R, Gumbsch P, Moseler M. Describing bond-breaking processes by reactive potentials: Importance of an environment-dependent interaction range. Phys Rev B 2008;78:161402. https://doi.org/10.1103/PhysRevB.78.161402.
[27] Wahnström G. Molecular-dynamics study of a supercooled two-component Lennard-Jones system. Phys Rev A 1991;44:3752–64. https://doi.org/10.1103/PhysRevA.44.3752.
[28] Yang Y, Shi Y. Single asperity friction in the wear regime. Friction 2018:1–7.
[29] Steeb S, Lamparter P. Structure of binary metallic glasses. J Non-Cryst Solids 156–158, Part 1993;1:24–33. https://doi.org/10.1016/0022-3093(93)90123-F.
[30] Giessen BC, Madhava M, Polk DE, Vander Sande J. Refractory amorphous inter-transition metal alloys. Mater Sci Eng 1976;23:145–50. https://doi.org/10.1016/0025-5416(76)90184-1.
[31] Hansen J-P, McDonald IR. Theory of Simple Liquids. Elsevier; 1990.
[32] Nosé S. A unified formulation of the constant temperature molecular dynamics methods. J Chem Phys 1984;81:511–9. https://doi.org/10.1063/1.447334.
[33] Hoover WG. Canonical dynamics: equilibrium phase-space distributions. Phys Rev A 1985;31:1695–7.
[34] Minsky H, Turner K. Achieving enhanced and tunable adhesion via composite posts. Appl Phys Lett 2015;106:201604.
[35] Zhang L, Jasa J, Gazonas G, Jérusalem A, Negahban M. Extracting continuum-like deformation and stress from molecular dynamics simulations. Comput Methods Appl Mech Eng 2015;283:1010–31.
[36] Yang J, Komvopoulos K. A stress analysis method for molecular dynamics systems. Int J Solids Struct 2020;193:98–105.
[37] Zhou M. A new look at the atomic level virial stress: on continuum-molecular system equivalence. Proc R Soc Lond Ser Math Phys Eng Sci 2003;459:2347–92.
[38] Yang J, Komvopoulos K. A molecular dynamics analysis of surface interference and tip shape and size effects on atomic-scale friction. J Tribol 2005;127:513–21. https://doi.org/10.1115/1.1843829.
[39] O'Hern CS, Liu AJ, Nagel SR. Effective temperatures in driven systems: static versus time-dependent relations. Phys Rev Lett 2004;93:165702. https://doi.org/10.1103/PhysRevLett.93.165702.
[40] Ono IK, O'Hern CS, Durian DJ, Langer SA, Liu AJ, Nagel SR. Effective temperatures of a driven system near jamming. Phys Rev Lett 2002;89:095703. https://doi.org/10.1103/PhysRevLett.89.095703.
[41] Xu N, O'Hern CS. Effective temperature in athermal systems sheared at fixed normal load. Phys Rev Lett 2005;94:055701. https://doi.org/10.1103/PhysRevLett.94.055701.
[42] Berthier L, Barrat J-L. Nonequilibrium dynamics and fluctuation-dissipation relation in a sheared fluid. J Chem Phys 2002;116:6228–42. https://doi.org/10.1063/1.1460862.
[43] Berthier L, Barrat J-L. Shearing a glassy material: numerical tests of nonequilibrium mode-coupling approaches and experimental proposals. Phys Rev Lett 2002;89:095702.
[44] D'Acunto M. Theoretical approach for the quantification of wear mechanisms on the nanoscale. Nanotechnology 2004;15:795. https://doi.org/10.1088/0957-4484/15/7/014.
[45] Ilg P, Barrat J-L. Driven activation vs. thermal activation, EPL. Europhys Lett 2007;79:26001. https://doi.org/10.1209/0295-5075/79/26001.
[46] Ilg P, Barrat J-L. Effective temperatures in a simple model of non-equilibrium, non-Markovian dynamics. In: J. Phys. Conf. Ser. IOP Publishing; 2006. p. 76.
[47] Shi Y, Katz MB, Li H, Falk ML. Evaluation of the disorder temperature and free-volume formalisms via simulations of shear banding in amorphous solids. Phys Rev Lett 2007;98:185505.
[48] Sang Y, Dubé M, Grant M. Thermal effects on atomic friction. Phys Rev Lett 2001;87:174301.
[49] Riedo E, Gnecco E, Bennewitz R, Meyer E, Brune H. Interaction potential and hopping dynamics governing sliding friction. Phys Rev Lett 2003;91:084502.
[50] Briscoe BJ, Evans DCB. The Shear Properties of Langmuir-Blodgett Layers. Proc R Soc Lond Math Phys Eng Sci 1982;380:389–407. https://doi.org/10.1098/rspa.1982.0048.
[51] Kurchan J. Emergence of macroscopic temperatures in systems that are not thermodynamical microscopically: towards a thermodynamical description of slow granular rheology. J Phys Condens Matter 2000;12:6611.
[52] Nowak ER, Knight JB, Ben-Naim E, Jaeger HM, Nagel SR. Density fluctuations in vibrated granular materials. Phys Rev E 1998;57:1971–82. https://doi.org/10.1103/PhysRevE.57.1971.
[53] Tambe NS, Bhushan B. Durability studies of micro/nanoelectromechanical systems materials, coatings and lubricants at high sliding velocities (up to 10mm/s) using a modified atomic force microscope. J Vac Sci Technol Vac Surf Films 2005;23:830–5. https://doi.org/10.1116/1.1843821.